



Inscription of Bragg gratings in undoped PMMA mPOF with Nd:YAG laser at 266 nm wavelength

Min, Rui; Pereira, Luis; Paixão, Tiago; Woyessa, Getinet; André, Paulo; Bang, Ole; Antunes, Paulo; Pinto, João; Li, Zhaohui; Ortega, Beatriz

Total number of authors:

11

Published in:

Optics Express

Link to article, DOI:

[10.1364/OE.27.038039](https://doi.org/10.1364/OE.27.038039)

Publication date:

2019

Document Version

Publisher's PDF, also known as Version of record

[Link back to DTU Orbit](#)

Citation (APA):

Min, R., Pereira, L., Paixão, T., Woyessa, G., André, P., Bang, O., Antunes, P., Pinto, J., Li, Z., Ortega, B., & Marques, C. (2019). Inscription of Bragg gratings in undoped PMMA mPOF with Nd:YAG laser at 266 nm wavelength. *Optics Express*, 27(26), 38039-38048. <https://doi.org/10.1364/OE.27.038039>

General rights

Copyright and moral rights for the publications made accessible in the public portal are retained by the authors and/or other copyright owners and it is a condition of accessing publications that users recognise and abide by the legal requirements associated with these rights.

- Users may download and print one copy of any publication from the public portal for the purpose of private study or research.
- You may not further distribute the material or use it for any profit-making activity or commercial gain
- You may freely distribute the URL identifying the publication in the public portal

If you believe that this document breaches copyright please contact us providing details, and we will remove access to the work immediately and investigate your claim.



Inscription of Bragg gratings in undoped PMMA mPOF with Nd:YAG laser at 266 nm wavelength

RUI MIN,^{1,2,3} LUIS PEREIRA,^{4,10} TIAGO PAIXÃO,⁴  GETINET WOYESSA,⁵  PAULO ANDRÉ,⁶  OLE BANG,^{5,7} PAULO ANTUNES,^{4,8}  JOÃO PINTO,⁴ ZHAOHUI LI,^{1,2} BEATRIZ ORTEGA,³ AND CARLOS MARQUES^{4,9} 

¹State Key Laboratory of Optoelectronic Materials and Technologies and School of Electronics and Information Technology, Sun Yat-sen University, 510275 Guangzhou, China

²Southern Laboratory of Ocean Science and Engineering (Guangdong, Zhuhai), 519000 Zhuhai, China

³ITEAM Research Institute, Universitat Politècnica de València, 46022 Valencia, Spain

⁴I3N & Physics Department, Universidade de Aveiro, 3810-193 Aveiro, Portugal

⁵DTU Fotonik, Department of Photonics Engineering, Technical University of Denmark, Denmark

⁶DETI and Instituto de Telecomunicações, Universidade de Aveiro, 3810-193 Aveiro, Portugal

⁷SHUTE Sensing Solutions A/S, Oldenvej 1A, 3490 Kvistgård, Denmark

⁸Instituto de Telecomunicações, Universidade de Aveiro, 3810-193 Aveiro, Portugal

⁹carlos.marques@ua.pt

¹⁰lmpereira@ua.pt

Abstract: We present the first Bragg gratings fabricated in two, three and five rings undoped PMMA microstructured polymer optical fibres (mPOFs) with relative low cost 266 nm Nd:YAG laser in the 850 nm region. The fibers were connectorised with commercial ferrules for easy coupling with silica patch cables. Temperature, humidity and strain sensitivities are measured and also the impact of ring structure and the diameter of POF on the characterization measurements are studied for potential applications. We also analyzed the effect of the number of hexagonal rings structure in gratings fabrication, noticing that larger number of rings lead to more difficulties to obtain strong gratings, where we consider this performance due to the scattering effects. We demonstrate Bragg gratings fabrication in 5-rings structure mPOF after 6 min by using 266 nm Nd:YAG laser whereas no Bragg gratings have been fabricated so far using 325 nm He-Cd laser system. Up to 30 dB relative reflected power gratings are obtained in two rings mPOF, showing good time stability and promising results for undoped mPOF applications.

© 2019 Optical Society of America under the terms of the [OSA Open Access Publishing Agreement](#)

1. Introduction

Polymer optical fibers (POFs) show a smaller Young's modulus and larger thermo-optic coefficient compared with silica counterparts, which make them suitable for different sensing scenarios. Bragg grating devices in POFs attracted huge attention driven by a wide range of sensing applications such as strain [1], temperature [1], humidity [2,3], liquid level [4] and ultrasounds [5]. The well-known biocompatibility also makes them as a promising sensing technology for biomedical and bioengineering industry [6–7].

The first poly (methyl methacrylate) (PMMA) polymer optical fiber Bragg grating (POFBG) was reported in 1999 by Peng's group [8]. Since then, great progress has been made in the POFBG fabrication. Different materials such as TOPAS [9–11], ZEONEX [12,13], CYTOP [14–15] or even polycarbonate [16–17] were introduced for different sensing modalities with unique advantages. However, until now, PMMA remains the preferred material for POFs composition. Moreover, different grating structures such as chirped [18–19], tilted [20], phase-shift [21] were investigated for sensing applications with optimal characteristics.

Due to the low photosensitivity of PMMA material, different kinds of dopants were used to improve the photosensitivity of the POF, such as benzyl dimethyl ketal (BDK) [22–23], or trans-4-stilbenemethanol (TS) [24] with the increase of the transmission loss as the main drawback. *Hu et al.* [25] mentioned the fiber loss of BDK doped mPOF is 100 times higher than the typical transmission loss of 2 dB/m at around 800 nm. Since the length is a critical issue for real sensing applications based on POFs, undoped PMMA mPOFs are more promising for real applications due to the low loss compared with doped PMMA mPOFs.

Besides the fiber materials and dopants, the irradiation laser system is also important for grating fabrication. Indeed, the research in this area has been very active since *Peng et al.* [8] used two illumination wavelengths (248 and 325 nm) for grating fabrication. Since then, continuous wave low power 325 nm light emitted by a He-Cd laser has been the preferred wavelength for fabrication of grating devices in POFs. Although several laser systems emitting light at different wavelengths were used for POF grating inscription, the fabrication of Bragg gratings in undoped POFs was demonstrated as a time-consuming process, i.e., 20 dB relative reflected signal was obtained in step index PMMA POF after a minimum time around 20 mins [26] whereas similar results were achieved in 3-rings mPOF around 7 mins [27]. However, Bragg grating devices were obtained using a 248 nm wavelength KrF system in less than 30 seconds [28] although this laser is bulky and expensive. Recently, *Pereira et al.* [29] demonstrated an 8 dB Bragg grating in BDK doped mPOF by using a single short pulse with low cost Nd:YAG laser at 266 nm. So far, no results have been achieved in undoped PMMA mPOFs.

In this paper, we present the first experimental results on Bragg gratings fabrication in undoped PMMA mPOFs with two, three and five hexagonal rings using a low cost Nd:YAG laser system operating at 266 nm wavelength. The impact of scattering in different hexagonal ring structures on UV fiber irradiation has been analyzed [30]. The characterization of the strain, temperature and humidity is also supplied for potential sensing applications.

2. Bragg gratings fabrication

In this work, three different kinds of undoped mPOF are used for gratings fabrication. They were all manufactured at *DTU Fotonik* by two steps method: 1) a PMMA rod is drilled with a predefined hole diameter and pitch, which is then drawn to a cane of smaller diameter; 2) the canes sleeved with PMMA tubes, resulting in a secondary preform that is drawn to a fiber. Figure 1(a)–1(c) shows the end faces of the two: Fig. 1(a), three: Fig. 1(b) and five: Fig. 1(c) hexagonal rings PMMA mPOFs. The average hole diameter and pitch of the fibers are 1.70 μm and 3.95 μm (2-rings), 1.90 μm and 4.60 μm (3-rings), 1.70 μm and 3.95 μm (5-rings), respectively. All samples were pre-annealed for 24 hours at 70 °C to reduce the internal stress in the fiber induced by the fabrication process. Moreover, due to the fabrication process, the diameter of fibers is not uniform since $\pm 5 \mu\text{m}$ diameter fluctuations were measured. More specifically, in this work the diameters of the employed fibers are 138 μm , 130 μm and 143 μm for the two, three and five-rings mPOFs, respectively (see Fig. 2). In order to fit each mPOF to the 125 μm diameter commercial ferrule, 2–3 cm length belong to the piece of mPOF was immersed in a tube full of acetone around 10 seconds, and we repeated the etching experiment in order to fit the ferrule correctly due to the uncertainty ($\pm 5 \mu\text{m}$ diameter fluctuations) about the diameter of each mPOF used. Note that the diameter of the three employed mPOFs are the same in Fig. 1(a)–1(c) due to the etching process to fit the 125 μm diameter commercial ferrule to connect into a standard single mode silica fiber patch cable, although the diameter of the fibers transversal sections is different for the three mPOFs, as shown in Fig. 2(a)–2(c).

A special room temperature cleaver [31] was used to cleave the samples, although core-shift could happen due to the one direction cleaver cut [32]; the polishing process was performed with a sandpaper to enhance the quality of the end face. One extra benefit about polishing is that avoids index matching gel going inside the holes of mPOF which affects the long-time stability

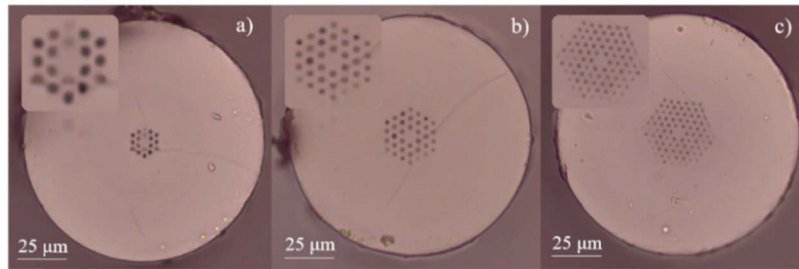


Fig. 1. End face of the different mPOF structures: (a) 2-rings, (b) 3-rings and (c) 5-rings. Insets: cross section of the microstructured region.

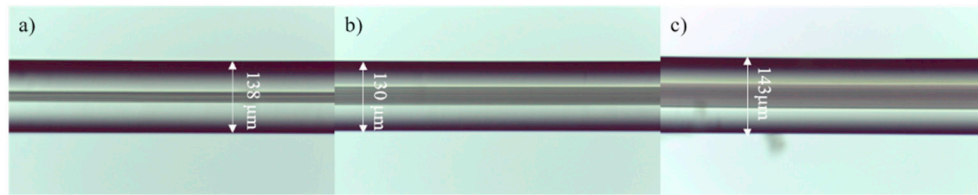


Fig. 2. Microscope images of the different mPOFs: (a) 2-rings, (b) 3-rings and (c) 5-rings.

of the gratings response. This gel is used in the connections of silica fiber and mPOF to avoid the formation of Fabry-Pérot cavities. Therefore, commercial ferrule technology provides easy connection with normal silica fiber patch cord, as shown in Fig. 3.

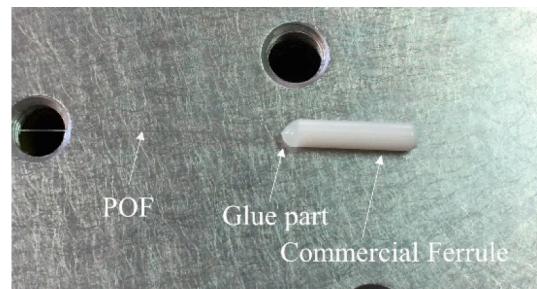


Fig. 3. Commercial ferrule connection technology for mPOF.

Figure 4 presents the grating devices inscription setup in undoped mPOFs. A pulsed Q-switched Nd:YAG laser system (LOTIS TII LS-2137U) emitting the fourth harmonic (266nm) was employed to produce the POFBGs, using emission power lamp energy of 24.6 J and measured pulse energy of 120 μ J with repetition rate of 5 Hz. The laser beam profile was circular with the diameter around 8 mm and divergence less than 1.0 mrad. The laser beam was focused onto the fiber core using a plano-convex cylindrical lens with effective focal length of 320 mm. The effective spot size of the beam on the fiber surface was 8 mm wide and 30 μ m high. The experimental setup was aligned and tested before the inscription in order to focus the UV beam onto the core of the fiber and obtain an effective POFBG inscription. The reflected spectrum was monitored using an 850 nm circulator, a super luminescent diode (Superlum SLD-371-HP1) and an optical spectrum analyzer (OSA Anritsu MS9740A). The phase mask employed was 10 mm long with a pitch of $\Lambda_{PM} = 567.8$ nm, designed for 248 nm irradiation.

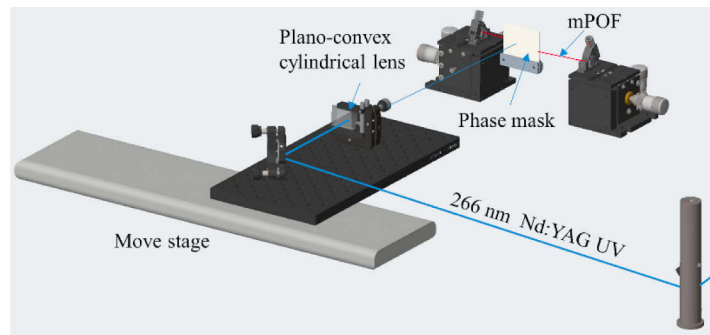


Fig. 4. Experimental setup for POFBG inscription using 266 nm Nd:YAG laser.

The reflected power was monitored during the Bragg gratings inscription in the three mPOFs described above, and an example of the reflected spectral power is shown in Fig. 5(a)–5(c) for each fiber. We obtained Bragg grating devices with 3 dB and 1 dB rejection in transmission for 2 and 3-rings mPOFs, respectively, but we could only measure the reflected power (17 dB above the noise level) for 5-rings mPOF and no transmission measurement was achieved considering the grating to be weak and, as is known, the scattering increases with the number of rings.

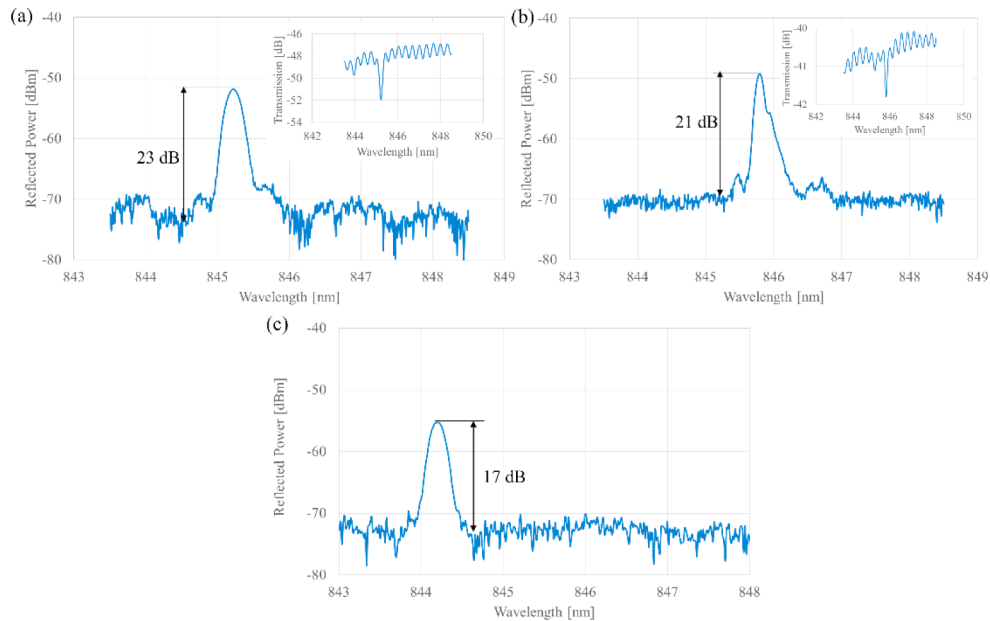


Fig. 5. Reflected spectral power of the Bragg grating in different mPOFs: (a) 2-rings, (b) 3-rings and (c) 5-rings. Insets in (a) and (b): transmission measurements.

During the inscription, the pulse energy and the orientation of the fiber were kept stable since the energy density in the core depends on the scattering arisen from the rings structure. Six gratings were fabricated to evaluate the angle effect on each mPOF structure [33]. Figure 6(a)–6(b) shows that the 2-rings mPOF presented the best result with the highest reflected power and the shortest time and 5-rings mPOF needed much more time for grating irradiation. However, no Bragg grating device has so far been reported in 5-rings structure mPOF using 325 nm He-Cd laser system, whereas we fabricated Bragg gratings in this fiber after 6 min by using 266 nm

Nd:YAG laser. Since a 248 nm KrF pulsed laser system allowed to shorten the irradiation time, as demonstrated by *Min et al.* [34] in doped step index POF, we tried 10 Hz frequency as the highest repetition rate of our Nd:YAG laser system using undoped two rings mPOF, and the shortest time was around 60 seconds with similar performance.

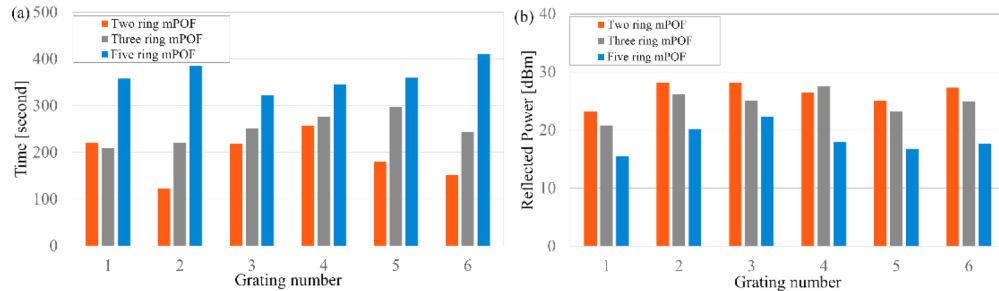


Fig. 6. Bragg grating devices in different PMMA mPOFs: (a) irradiation time, (b) reflected power.

In the fabricated POFBGs, the central wavelength blue-shifted after removing the fibers from the clamps of the inscription setup since the fiber was subjected to small strain during the inscription [35]. Three samples were monitored during two weeks, as shown in Fig. 7, and the reflected power of all gratings suffered a significant decrease during the second day, but then they kept stable over time. After 14 days, the reflected power decreased about 6 dB for 2-rings and 5-rings, and about 7.5 dB for 3-rings mPOF, although gratings in all the fibers exhibited the same decay characteristic.

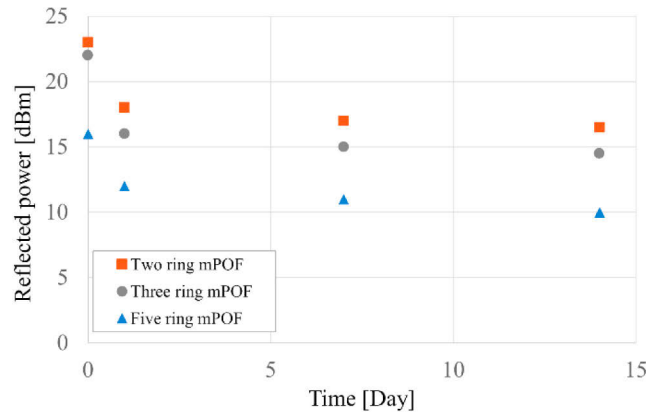


Fig. 7. Reflected peak power of grating inscribed into two, three and five rings mPOF over time.

In order to obtain strong and stable gratings over time, we aimed to fabricate gratings in 2-rings mPOF with strong reflected signal. As it was referenced before, the position of the mPOF is important since the energy density of the UV beam in the core position may be affected by the microstructures located on the beam path [33]. This means that very strong gratings in mPOF can only be achieved sometimes. Figure 8(a) shows the reflected power evolution of one grating during the inscription in 2-rings mPOF. The experimental setup was the same as before, using the pulsed Q-switched Nd:YAG laser system with pump lamp energy of 24.6 J and repetition rate of 6 Hz. After 15 minutes of laser exposure, when the grating stopped growing, the POFBG showed 36.5 dB relative reflected power. The POFBG was monitored during 30 days and, as

Fig. 8(b) shows, the reflected power decreased about 3.6 dB. These results show that strong gratings can be achieved using this laser system, being also more stable in time, in this case with a reflected peak above 30 dB after 30 days.

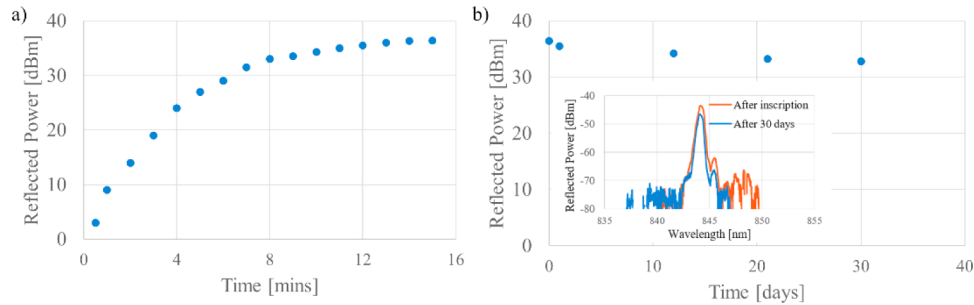


Fig. 8. Reflected power evolution for 2-rings mPOF: (a) during inscription and (b) during 30 days after inscription (Inset: reflected power spectra of the POFBG just after the inscription and after 30 days).

3. Temperature, strain and humidity performance

In this section, we report the full characterization of the Bragg gratings in different mPOFs in terms of temperature, strain and humidity. Temperature sensitivity of the gratings was measured by using a Peltier plate which contains a small v-groove where the temperature is set with a thermo-electric controller. Silicone grease was placed on the grating position to increase temperature conduction. The central wavelength of the grating was measured from 22°C to 52°C, in 5°C steps with 10 mins waiting time for thermal stabilization. The obtained thermal sensitivities were -39.4 ± 2.0 pm/°C, -44.9 ± 2.0 pm/°C and -47 ± 2.0 pm/°C for 2-rings (1.16 nm shift), 3-rings (1.34 nm shift) and 5-rings (1.36 nm shift), respectively, as shown in Fig. 9. The results were slightly higher than those measured in [36], probably due to the different pre-annealing method. The experimental results show the temperature sensitivity is dependent on the diameter and the number of rings of the mPOFs.

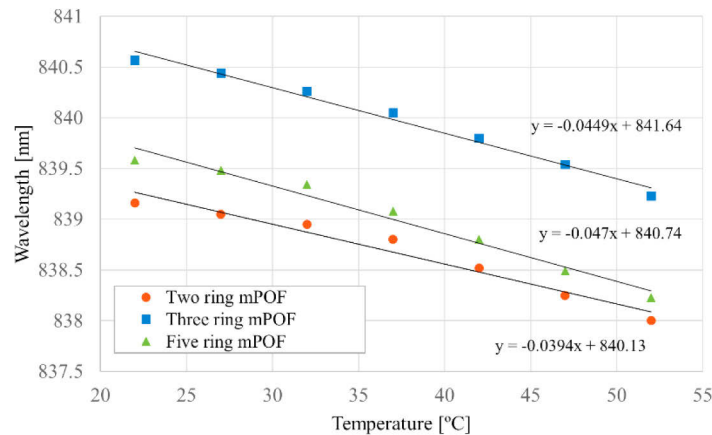


Fig. 9. POFBG central wavelength under different temperatures.

In order to characterize the strain sensitivity of the fabricated gratings, a 11.61 cm long fiber containing the grating was fixed between two X-Y-Z moveable stages by using flexure stage

accessories (Thorlabs HFF001). The fiber was strained step-by-step with 5 min waiting time between each step at room temperature. As Fig. 10 shows, the computed strain sensitivities from a linear regression of the raw data were 0.71 ± 0.05 pm/ $\mu\epsilon$, 0.75 ± 0.05 pm/ $\mu\epsilon$ and 0.74 ± 0.05 pm/ $\mu\epsilon$ for 2, 3 and 5-rings mPOFBGs, respectively. The small differences in strain sensitivities between different mPOFs are directly related to the fiber diameter since the three rings mPOF has a smaller diameter (130 μm) and higher sensitivity [37]. Moreover, by comparing the two and five rings mPOF with 138 μm and 143 μm diameters; the former has the lowest sensitivity due to the combined effect of large diameter and less holes. Nevertheless, our results are similar to those previously reported in three rings mPOF Bragg gratings [38]. Also, we can consider that the values are equal within experimental uncertainty.

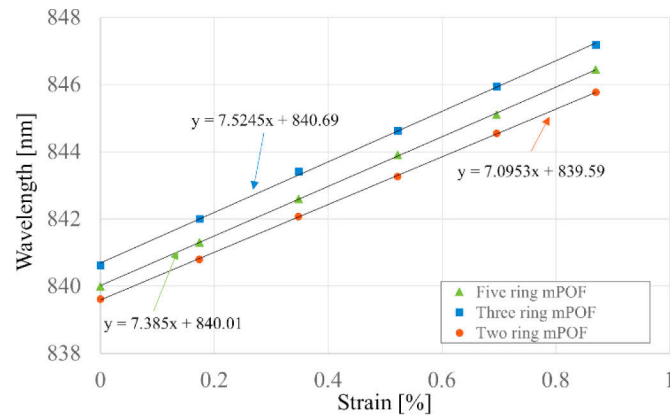


Fig. 10. Central wavelength of the gratings under different strain levels.

Finally, all gratings were placed into a climate chamber (Angelantoni Industrie CH340) at a constant temperature of 22°C and 30% of relative humidity (RH) during 100 min for stabilization. Then, the RH was increased up to the value of 90% in 20% steps, waiting 100 min between each step. The reflected spectrum was monitored using an 850 nm circulator, a super luminescent diode (Superlum SLD-371-HP1) and an optical spectrum analyzer (Yokogawa AQ6373B). Figure 11(a)–11(c) shows the central wavelength shift and the time humidity change. The computed humidity sensitivities from a linear regression of the raw data were equal to 30.3 ± 0.005 pm/%, 27.0 ± 0.005 pm/% RH and 30.2 ± 0.005 pm/% RH for 2, 3 and 5 rings mPOFBGs, respectively. Once again, the diameter and the number of the microstructure holes may have influence in those measurements where the 3-rings mPOF has the lowest sensitivity. Also, Fig. 11(a)–11(c) indicates that both 2 and 5-rings mPOFs need more time for humidity stabilization when compared with three rings mPOF, possibly due to the higher fiber diameter. With the same diameter of mPOF, if we increase the ring structure, it means use less material for mPOF the strain sensitivity could increase. Increasing the diameter (more material used) the strain sensitivity decreases. The temperature and humidity sensitivities are more related with the material itself (e.g. diameter, number of rings, and ring structure).

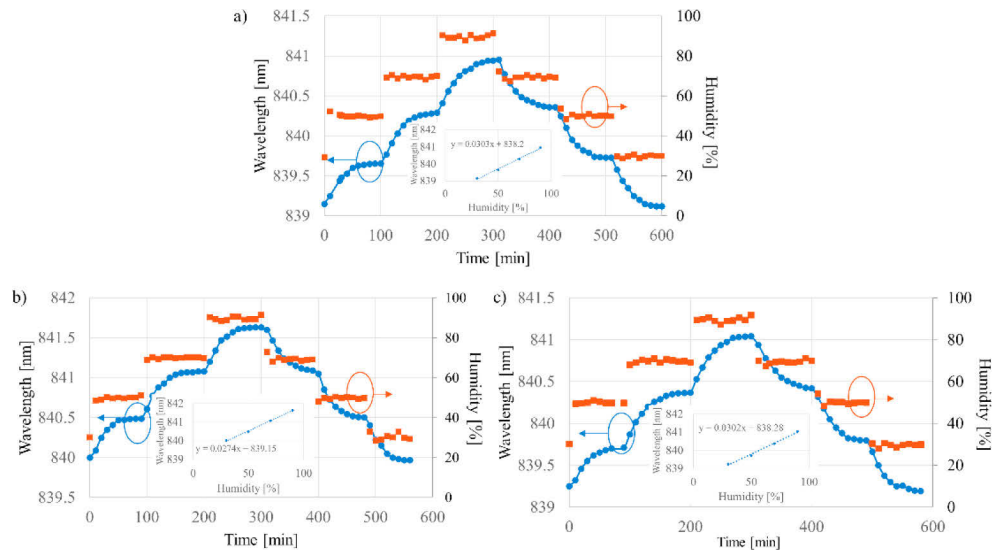


Fig. 11. Wavelength and humidity monitoring during time for different mPOFs: a) 2-rings mPOF, b) 3-rings mPOF and c) 5-rings mPOF (Inset: Wavelength vs Humidity).

4. Conclusion

In this work, to the best of the author's knowledge, we have presented the first inscription of Bragg gratings in different rings structure undoped PMMA mPOFs at low loss 850 nm region with a relative low cost 266 nm wavelength Nd:YAG laser system. The gratings were inscribed in two, three and five hexagonal rings, showing better results in two rings mPOF, since it has less microstructure holes in the laser beam path. Although some gratings may lack stability in time, this laser leads to obtain strong and stable gratings with more than 30 dB relative reflected power for 30 days. These results represent a significant progress in POFBG technology since our approach combines cheap and low loss undoped mPOF with low cost and easy operation laser for grating production. Temperature, strain and humidity sensitivities have been also measured and discussed referring to the diameter and number of rings of the fibers, indicating that the 2-rings mPOF with 138 μm diameter showed the lowest sensitivity in temperature as $-39.4 \pm 2.0 \text{ pm}/^\circ\text{C}$ and strain as $0.71 \pm 0.05 \text{ pm}/\mu\epsilon$. And 3-rings mPOF with 130 μm diameter showed shortest time for humidity stabilization. Furthermore, the use of this laser has allowed to fabricate gratings in 5-rings mPOF, whereas this has not been demonstrated yet by using 325 nm He-Cd laser system.

Funding

Ministerio de Ciencia, Innovación y Universidades (RTI2018-101658-B-I00); Fundação para a Ciência e a Tecnologia (PD/BD/128265/2016, UID/CTM/50025/2019, UID/EEA/50008/2019); National Natural Science Foundation of China (61435006, 61525502); Science and Technology Planning Project of Guangdong Province (2017B010123005, 2018B010114002); Local Innovation and Research Teams Project of Guangdong Pearl River Talents Program (2017BT01X121).

Acknowledgments

This work is also funded by national funds (OE), through FCT – Fundação para a Ciência e a Tecnologia, I.P., in the scope of the framework contract foreseen in the numbers 4, 5 and 6 of the article 23, of the Decree-Law 57/2016, of August 29, changed by Law 57/2017, of July 19.

Disclosures

The authors declare no conflicts of interest.

References

1. D. J. Webb, "Fibre Bragg grating sensors in polymer optical fibres," *Meas. Sci. Technol.* **26**(9), 092004 (2015).
2. W. Zhang, D. J. Webb, and G.-D. Peng, "Investigation into time response of polymer fiber Bragg grating based humidity sensors," *J. Lightwave Technol.* **30**(8), 1090–1096 (2012).
3. G. Woyessa, K. Nielsen, A. Stefani, C. Markos, and O. Bang, "Temperature insensitive hysteresis free highly sensitive polymer optical fiber Bragg grating humidity sensor," *Opt. Express* **24**(2), 1206–1213 (2016).
4. C. Marques, G.-D. Peng, and D. J. Webb, "Highly sensitive liquid level monitoring system utilizing polymer fiber Bragg gratings," *Opt. Express* **23**(5), 6058–6072 (2015).
5. C. Broadway, G. Woyessa, O. Bang, P. Mégret, and C. Caucheteur, "An L-band ultrasonic probe using polymer optical fibre," *Photons Plus Ultrasound: Imaging and Sensing 2019*. Vol. 10878. International Society for Optics and Photonics.
6. K. Peters, "Polymer optical fiber sensors—A review," *Smart Mater. Struct.* **20**(1), 013002 (2011).
7. J. Bonafacino, H. Y. Tam, T. S. Glen, X. Cheng, C. F. J. Pun, J. Wang, P. H. Lee, M. L. V. Tse, and S. T. Boles, "Ultra-fast polymer optical fibre Bragg grating inscription for medical devices," *Light: Sci. Appl.* **7**(3), 17161 (2018).
8. Z. Xiong, G. D. Peng, B. Wu, and P. L. Chu, "Highly tunable Bragg gratings in single-mode polymer optical fibers," *IEEE Photonics Technol. Lett.* **11**(3), 352–354 (1999).
9. W. Yuan, L. Khan, D. J. Webb, K. Kalli, H. K. Rasmussen, A. Stefani, and O. Bang, "Humidity insensitive TOPAS polymer fiber Bragg grating sensor," *Opt. Express* **19**(20), 19731–19739 (2011).
10. C. Markos, A. Stefani, K. Nielsen, H. K. Rasmussen, W. Yuan, and O. Bang, "High-Tg TOPAS microstructured polymer optical fiber for fiber Bragg grating strain sensing at 110 degrees," *Opt. Express* **21**(4), 4758–4765 (2013).
11. G. Woyessa, A. Fasano, A. Stefani, C. Markos, K. Nielsen, H. K. Rasmussen, and O. Bang, "Single mode stepindex polymer optical fiber for humidity insensitive high temperature fiber Bragg grating sensors," *Opt. Express* **24**(2), 1253–1260 (2016).
12. G. Woyessa, A. Fasano, C. Markos, A. Stefani, H. K. Rasmussen, and O. Bang, "Zeonex microstructured polymer optical fiber: Fabrication friendly fibers for high temperature and humidity insensitive Bragg grating sensing," *Opt. Mater. Express* **7**(1), 286–295 (2017).
13. G. Woyessa, J. K. M. Pedersen, A. Fasano, K. Nielsen, C. Markos, H. K. Rasmussen, and O. Bang, "Zeonex-PMMA microstructured polymer optical FBGs for simultaneous humidity and temperature sensing," *Opt. Lett.* **42**(6), 1161–1164 (2017).
14. A. Lacraz, M. Polis, A. Theodosiou, C. Koutsides, and K. Kalli, "Femtosecond laser inscribed Bragg gratings in low loss CYTOP polymer optical fiber," *IEEE Photonics Technol. Lett.* **27**(7), 693–696 (2015).
15. R. Min, B. Ortega, A. Leal-Junior, and C. Marques, "Fabrication and characterization of Bragg grating in CYTOP POF at 600-nm wavelength," *IEEE Sens. Lett.* **2**(3), 1–4 (2018).
16. G. Woyessa, A. Fasano, C. Markos, H. K. Rasmussen, and O. Bang, "Low loss polycarbonate polymer optical fiber for high temperature FBG humidity sensing," *IEEE Photonics Technol. Lett.* **29**(7), 575–578 (2017).
17. A. Fasano, G. Woyessa, P. Stajanca, C. Markos, A. Stefani, K. Nielsen, H. K. Rasmussen, K. Krebber, and O. Bang, "Fabrication and characterization of polycarbonate microstructured polymer optical fibers for high-temperature-resistant fiber Bragg grating strain sensors," *Opt. Mater. Express* **6**(2), 649–659 (2016).
18. R. Min, B. Ortega, and C. Marques, "Fabrication of tunable chirped mPOF Bragg gratings using a uniform phase mask," *Opt. Express* **26**(4), 4411–4420 (2018).
19. R. Min, B. Ortega, C. Broadway, C. Caucheteur, G. Woyessa, O. Bang, P. Antunes, and C. Marques, "Hot water-assisted fabrication of chirped polymer optical fiber Bragg gratings," *Opt. Express* **26**(26), 34655–34664 (2018).
20. X. Hu, C. F. J. Pun, H. Y. Tam, P. Mégret, and C. Caucheteur, "Tilted Bragg gratings in step-index polymer optical fiber," *Opt. Lett.* **39**(24), 6835–6838 (2014).
21. L. Pereira, A. Pospori, P. Antunes, M. F. Domingues, S. Marques, O. Bang, D. J. Webb, and C. A. F. Marques, "Phase-shifted Bragg grating inscription in PMMA microstructured POF using 248-nm UV radiation," *J. Lightwave Technol.* **35**(23), 5176–5184 (2017).
22. Y. Luo, Q. Zhang, H. Liu, and G. D. Peng, "Gratings fabrication in benzildimethylketal doped photosensitive polymer optical fibers using 355 nm nanosecond pulsed laser," *Opt. Lett.* **35**(5), 751–753 (2010).
23. D. Sáez-Rodríguez, K. Nielsen, H. K. Rasmussen, O. Bang, and D. J. Webb, "Highly photosensitive polymethyl methacrylate microstructured polymer optical fiber with doped core," *Opt. Lett.* **38**(19), 3769–3772 (2013).
24. J. Yu, X. Tao, and H. Tam, "Trans-4-stilbenemethanol-doped photosensitive polymer fibers and gratings," *Opt. Lett.* **29**(2), 156–158 (2004).
25. X. Hu, G. Woyessa, D. Kinet, J. Janting, K. Nielsen, O. Bang, and C. Caucheteur, "BDK-doped core microstructured PMMA optical fiber for effective Bragg grating photo-inscription," *Opt. Lett.* **42**(11), 2209–2212 (2017).
26. C. A. F. Marques, L. B. Bilro, N. J. Alberto, D. J. Webb, and R. N. Nogueira, "Narrow bandwidth Bragg gratings imprinted in polymer optical fibers for different spectral windows," *Opt. Commun.* **307**, 57–61 (2013).
27. I.-L. Bundalo, K. Nielsen, C. Markos, and O. Bang, "Bragg grating writing in PMMA microstructured polymer optical fibers in less than 7 minutes," *Opt. Express* **22**(5), 5270–5276 (2014).

28. R. Oliveira, L. Bilro, and R. Nogueira, "Bragg gratings in a few mode microstructured polymer optical fiber in less than 30 seconds," *Opt. Express* **23**(8), 10181–10187 (2015).
29. L. Pereira, R. Min, X. Hu, C. Caucheteur, O. Bang, B. Ortega, C. Marques, P. Antunes, and J. L. Pinto, "Polymer optical fiber Bragg grating inscription with a single Nd: YAG laser pulse," *Opt. Express* **26**(14), 18096–18104 (2018).
30. C. A. F. Marques, R. Min, A. Leal Junior, P. Antunes, A. Fasano, G. Woyessa, K. Nielsen, H. K. Rasmussen, B. Ortega, and O. Bang, "Fast and stable gratings inscription in POFs made of different materials with pulsed 248 nm KrF laser," *Opt. Express* **26**(2), 2013–2022 (2018).
31. D. Sáez-Rodríguez, R. Min, B. Ortega, K. Nielsen, and D. J. Webb, "Passive and portable polymer optical fiber cleaver," *IEEE Photonics Technol. Lett.* **28**(24), 2834–2837 (2016).
32. A. Stefani, K. Nielsen, H. K. Rasmussen, and O. Bang, "Cleaving of TOPAS and PMMA microstructured polymer optical fibers: Core-shift and statistical quality optimization," *Opt. Commun.* **285**(7), 1825–1833 (2012).
33. I. L. Bundalo, K. Nielsen, and O. Bang, "Angle dependent Fiber Bragg grating inscription in microstructured polymer optical fibers," *Opt. Express* **23**(3), 3699–3707 (2015).
34. R. Min, B. Ortega, X. Hu, C. Broadway, C. Caucheteur, C. F. Jeff Pun, H. Y. Tam, P. Antunes, and C. Marques, "Bragg gratings inscription in TS-doped PMMA POF by using 248-nm KrF pulses," *IEEE Photonics Technol. Lett.* **30**(18), 1609–1612 (2018).
35. W. Yuan, A. Stefani, and O. Bang, "Tunable polymer Fiber Bragg Grating (FBG) inscription: Fabrication of dual-FBG temperature compensated polymer optical fiber strain sensors," *IEEE Photonics Technol. Lett.* **24**(5), 401–403 (2012).
36. J. Janting, J. Pedersen, R. Inglev, G. Woyessa, K. Nielsen, and O. Bang, "Effects of Solvent Etching on PMMA Microstructured Optical Fiber Bragg Grating," *J. Lightwave Technol.* **37**(18), 4469–4479 (2019).
37. A. Stefani, S. Andresen, W. Yuan, N. Herholdt-Rasmussen, and O. Bang, "High Sensitivity Polymer Optical Fiber-Bragg-Grating-Based Accelerometer," *IEEE Photonics Technol. Lett.* **24**(9), 763–765 (2012).
38. A. Pospori, C. A. F. Marques, D. Sáez-Rodríguez, K. Nielsen, O. Bang, and D. J. Webb, "Thermal and chemical treatment of polymer optical fiber Bragg grating sensors for enhanced mechanical sensitivity," *Opt. Fiber Technol.* **36**, 68–74 (2017).